Electrocatalytic Scission of Unactivated C(sp^3)−C(sp^3) Bonds Through Real-Time Manipulation of Surface-Bound Intermediates

*Harshal B. Bakshi[1]‡, Christine Lucky[1]‡, Hsiang-Sheng Chen[1], Marcel Schreier[1,2]**

[1] Department of Chemical and Biological Engineering, University of Wisconsin-Madison, Madison, Wisconsin 53706, United States

[2] Department of Chemistry, University of Wisconsin-Madison, Madison, Wisconsin 53706, United States

‡ These authors contributed equally.

Corresponding Author

* Prof. Marcel Schreier

Department of Chemical and Biological Engineering & Department of Chemistry

University of Wisconsin – Madison

1415 Engineering Drive, Madison, WI 53706

E-mail: mschreier2@wisc.edu

ABSTRACT

We demonstrate an electrocatalytic approach to cleave the C(sp^3)−C(sp^3) bond in ethane at room temperature. This reaction is enabled by time-dependent electrode potential sequences, combined with monolayer-sensitive in-situ analysis, which allows us to gain independent control over ethane adsorption, C−C bond fragmentation, and methane desorption. Importantly, our approach allowed us to vary the electrode potential to promote the fragmentation of ethane *after it is bound to the catalyst surface*, resulting in unprecedented control over the selectivity of this alkane transformation reaction. Steering the transformation of intermediates after adsorption constitutes an underexplored lever of control in catalysis. As such, our findings widen the parameter space for catalytic reaction engineering and open the door to future sustainable synthesis and energy storage technologies.

TOC FIGURE

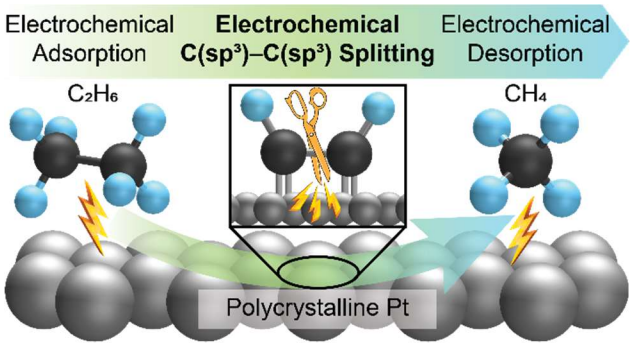

Introduction

Electrocatalysis plays a critical role in future technologies for energy storage and sustainable synthesis. For example, the past decade has seen astonishing advances in the electricity-driven production of synthetic fuels and chemicals from CO_2,[1,2] the renewable synthesis of NH_3,[3,4] and the sustainable production of crucial platform and fine chemicals.[5–9] Beyond simply coupling chemical transformations with renewable electricity, however, the unique features of electrochemical driving forces also hold the promise of enabling novel types of reactivity.

For example, in classical thermal catalysis, the outcome of a reaction is predetermined by the properties of the active site and its microenvironment.[10,11] Electrocatalysis offers an additional lever of control by allowing changes to the potential *during a catalytic reaction,* thereby dynamically adapting the environment to the requirements of individual reaction steps.[12–17] This idea has been exploited to improve the rate and selectivity of reactions such as formic acid oxidation[12] and CO_2 reduction,[18] by applying rapidly oscillating potentials to electrodes. However, while potential variations have been used to enhance well-established electrocatalytic reactions which can occur under constant electrochemical bias, they have not been used to enable electrocatalytic reactions *which are inaccessible through the application of static potentials*. In addition, it remains an open question whether time-dependent potentials are able to transform catalytic adsorbates *while they are bound to the catalyst surface*. Addressing both challenges requires an experimental strategy which can provide real-time insight into the impact of time-dependent modifications of the potential on the transformation catalytic intermediates.

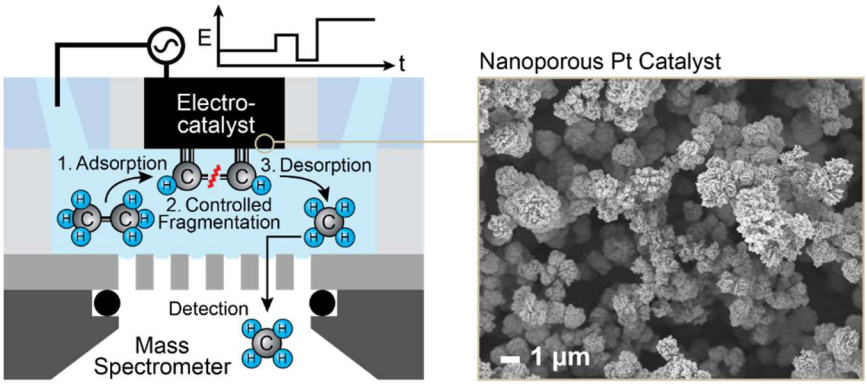

Figure 1. Schematic of the EC-MS analysis method to perform stepwise analysis of C−C scission reactions and structure of the platinized Pt electrode.

Herein, we realize the advantages of time-dependent potentials to enable a reaction that cannot be performed at constant voltages. Specifically, we demonstrate the electrocatalytic fragmentation of ethane to methane at room temperature. Using real-time analysis by electrochemical mass spectrometry (EC-MS), [19,20] we observed the products generated following a series of potential steps leading to the fragmentation of ethane. Our experiments allowed us to gain independent control over the adsorption of ethane, fragmentation of its $C(sp^3)$–$C(sp^3)$ bond, and the desorption of methane using only the applied potential as control handle (**Figure 1**). Our work is inspired by investigations into hydrocarbon fuel cells in the 1960s that demonstrated that alkanes can be

electrochemically oxidized to CO_2 at temperatures below 100° C, which involved the cleaving of C–C bonds.[21–29] This demonstrates that C–H and C–C bonds can be electrocatalytically activated near room temperature, a surprising fact, given that temperatures of 300 - 400° C are required to drive the same reactions on Pt in thermal chemistry.[30] We build on these findings to gain independent control of the adsorption, desorption, and transformation of adsorbed catalytic intermediates. Specifically, we demonstrate that the fragmentation of $C(sp^3)$−$C(sp^3)$ bonds is promoted by oxidative potentials and that fragmentation can be initiated by potential changes applied *while intermediates are bound to the surface*. As such, our results open the path to the room-temperature electrochemical activation of challenging substrates such as alkanes. We believe that the impact of our results transcends the electrocatalytic fragmentation of C–C bonds as gaining independent control over each elementary step of a catalytic reaction holds the promise to seed broadly applicable methodologies to enable novel electrocatalytic transformations.

Controlling ethane adsorption and product desorption through electrochemical potentials.
In a first step, we investigated the ability of electrochemical potentials to precisely control the adsorption of substrates and desorption of products from an electrocatalyst surface. We used electrochemical mass spectrometry (**Figure 1**) to investigate the impact of applied potentials on catalytic adsorption, transformation, and desorption steps. In EC-MS, an electrode-electrolyte interface is brought into close contact with the inlet of a mass-spectrometer, allowing for the real-time detection of sub-monolayers of gaseous products desorbing from the electrode.[19] To investigate the impact of applied potentials on ethane adsorption, we measured the total amount of ethane adsorbed to a platinized Pt electrode (Figures S1-S3, Table S1) in 1 M H_2SO_4 at potentials between 0.1 and 0.7 V (all potentials are reported *vs* the reversible hydrogen electrode [RHE]). Our data shows that the adsorption of ethane reaches a maximum of 49 nmol cm^{-2} at 0.3 V (Figure S4). The total adsorption of ethane decreases nearly symmetrically as the potential deviates from 0.3 V and at 0.1 and 0.7 V only trace ethane was adsorbed. This behavior agrees with previous voltammetric studies of ethane adsorption[22,25,26,28], which show that adsorption is maximized at 0.3 - 0.4 V, near the potential of zero charge (PZC) of Pt in sulfuric acid solutions.[25,28,29,31]
Analogous to ethane adsorption, we used variations in potential to control the desorption of hydrocarbon products from the electrode surface. Alkyl fragments have been reported to desorb from Pt as alkanes at cathodic potentials, where the generation of surface-hydrogen atoms facilitates their hydrogenation to saturated hydrocarbons.[18–23,29] To verify this, we adsorbed ethane at 0.3 V for 30 min, then removed residual substrate by purging the cell with He while maintaining the same potential. We subsequently changed the potential to a more reducing value (0.05 V) to desorb surface-adsorbed alkyl intermediates as saturated hydrocarbons.[26] Upon desorption, we detected the release of ethane. These tests confirm that alkanes can be independently adsorbed to and desorbed from a Pt electrode surface at room temperature under the sole control of the applied potential. Importantly, when measuring the desorption of adsorbed ethane, *we also detected significant amounts of methane*. In fact, when ethane was adsorbed at 0.3 V, we found that methane made up most of the reductively desorbed species (**Figure 2**).

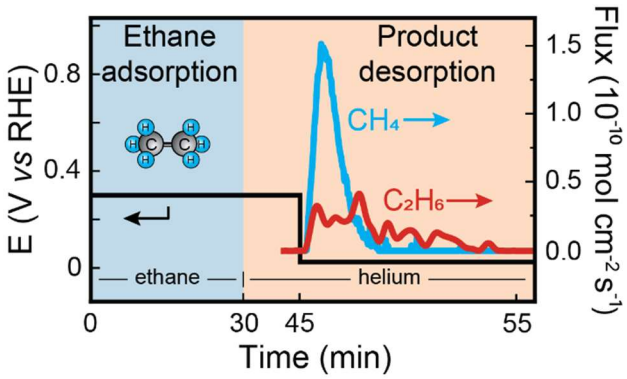

Figure 2. Potential program for 0.3 V adsorption of ethane, along with detected MS signals for methane and ethane.

The observation of methane generation from ethane at room temperature highlights that $C(sp^3)–C(sp^3)$ splitting can take place under mild conditions at an electrode surface. As such, it stands in contrast to classical thermocatalysis, where alkane fragmentation requires high temperatures to occur,[30] and indicates that electrocatalysis under time-dependent potentials provides unique routes to alkane transformations. This observation raises the question whether the applied potentials provide control over the ethane fragmentation process, which we address next.

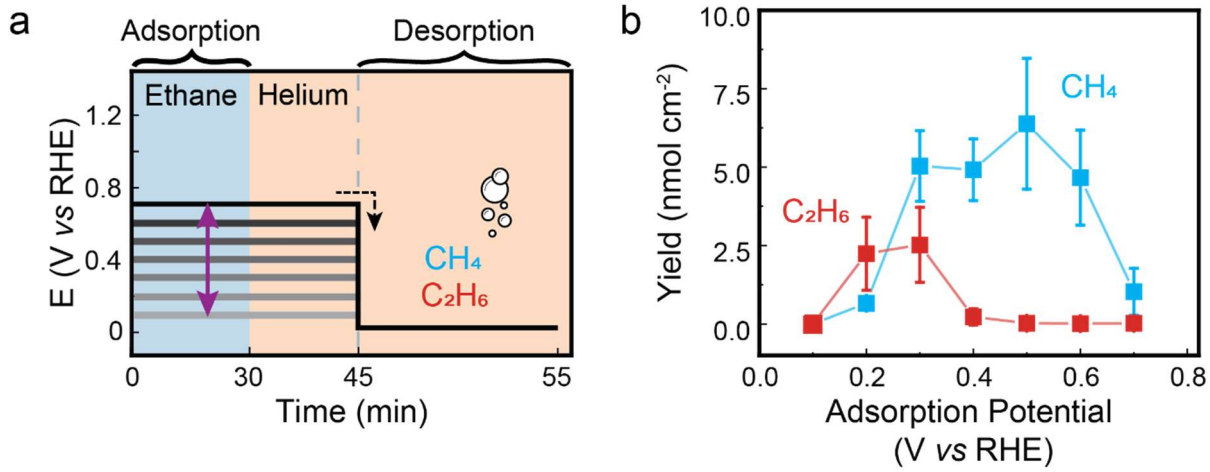

Figure 3. (a) Potential program for 0.1-0.7 V adsorption of ethane. **(b)** Potential dependent yields of methane and ethane upon reductive desorption. Points are the average of at least 3 trials and error bars indicate 1 std. dev.

We found that the selectivity towards C–C bond fragmentation, in other words the ratio between methane and ethane products, depends on the potential applied during adsorption. To investigate this phenomenon, we varied the ethane adsorption potential from 0.1 V to 0.7 V, while keeping all other parameters constant (**Figure 3a**). Ethane was only desorbed in appreciable quantities following adsorption at 0.2 and 0.3 V as seen in **Figure 3b**. The yield of methane, however, increased sharply from 0.2 to 0.3 V and remained approximately constant until dropping at 0.7 V, which is driven by low total adsorption (Figure S4). Moreover, the sharp increase in methane and decrease in ethane over a narrow potential range around 0.3 V points to a specific threshold potential necessary for C–C bond scission to occur. It is interesting to note that both ethane adsorption and product desorption occur at potentials that are well within the stability window of

aqueous environments (0 – 1.23 V). Therefore, hydrogen evolution and oxygen evolution are not competing with any of the steps involved in room temperature ethane fragmentation.

Electrochemical potentials yield independent control of ethane adsorption and fragmentation.

To determine whether C−C bond fragmentation occurs upon adsorption or after alkanes are bound to the surface, we investigated the impact of applied electrochemical potentials on *ethane already adsorbed to the electrode*. We first adsorbed ethane at 0.2 V, where it undergoes minimal fragmentation. Excess ethane was then removed from the cell by purging with helium and the potential was stepped to 0.5 V for different amounts of time, ranging from 1 to 15 minutes. Subsequently, alkanes were released from the surface by reductive desorption at 0.05 V (**Figure 4a**).

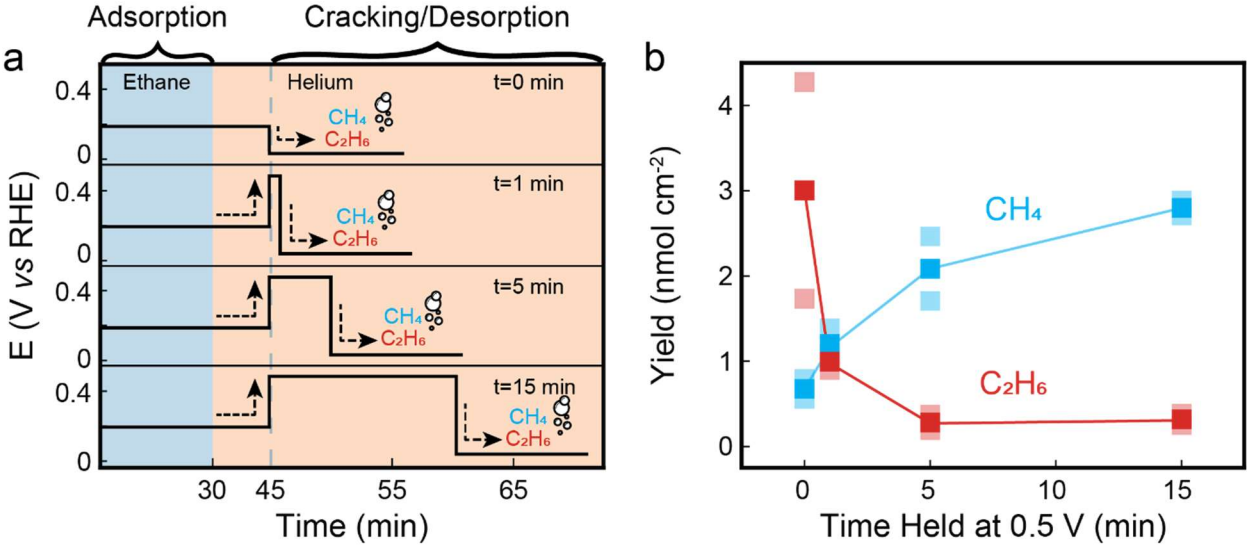

Figure 4. (a) Potential program for adsorption at 0.2 V followed by a step to 0.5 V for 0-15 min and subsequent reductive desorption at 0.05 V. The standard oxidative hold at 1.2 V was applied after the shown sequence to quantify remaining organic surface species. **(b)** Methane and ethane yields upon reductive desorption after holds at 0.5 V of varying lengths. Light blue and light red points correspond to methane and ethane yields, respectively. Darker points correspond to the average of their lighter counterparts.

Our data shows that increasing the potential after adsorption triggers C−C scission in the surface-bound ethane. Upon stepping the potential from 0.2 V to 0.5 V, we observed a decrease in ethane and an increase in methane yield (**Figure 4b**), demonstrating that ethane adsorption and C−C bond breaking happen in distinct steps that can be independently controlled. Varying the length of the 0.5 V hold revealed that methane generation increases over time, indicating that the selectivity can be controlled through the duration for which oxidative potentials are applied. The fact that adsorption and C−C fragmentation occur independently from each-other opens the door to use the magnitude of the applied potential to control the fragmentation of intermediates while they are bound to the surface. To verify this premise, we again adsorbed ethane at 0.2 V, where it undergoes minimal fragmentation, and subsequently applied varying oxidative potentials for 5 min prior to product desorption (**Figure 5a,** Figure S5).

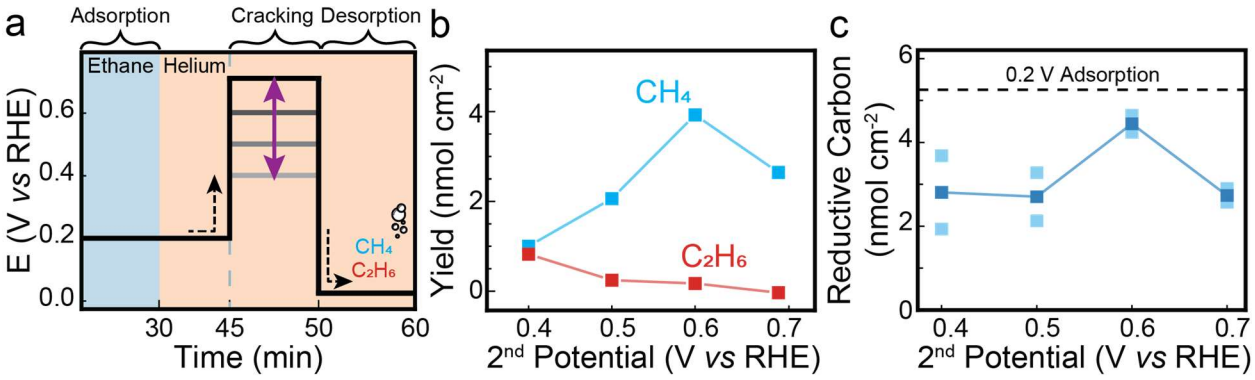

Figure 5. (a) Schematic of the double potential program. The standard oxidative hold at 1.2 V was applied after the shown sequence to quantify remaining organic surface species. **(b)** Yield of methane and ethane for the double potential experiments. Data corresponds to the average of two replicates and the raw data is shown in Figure S8. **(c)** Yield of reductively desorbed carbon for the double potential experiments. The dashed line indicates the reductive carbon desorbed after adsorption at 0.2 V in the absence of a second potential hold. The lighter points represent individual trials and the darker points are the corresponding average values.

We found that increasing the applied potential from 0.4 to 0.6 V leads to an increase in methane formation with a maximum at 0.6 V (**Figure 5b**). At 0.7 V, methane generation decreased, coinciding with measurable CO_2 generation during the oxidative hold (Figure S6). We therefore ascribe this decrease to the competitive oxidation of adsorbed alkanes at highly oxidizing potentials, which was also observed to a lesser extent at 0.6 V (Figure S7).

Our findings provide direct evidence that the electrochemical potential can serve as a handle to steer the transformation of surface intermediates while they are bound to the electrode surface. The ability to control the amount and selectivity of alkanes released by applying electrochemical potentials to alkane-covered electrodes highlights the unique opportunity electrochemistry provides to steer the reactivity of surface bound intermediates and enable new types of chemistry that are not readily available under thermochemical conditions and in electrocatalysis under constant potential.

For example, the ability to separate the conditions for ethane adsorption from the conditions needed for its fragmentation allowed us to independently tune each elementary step involved in C–C bond fragmentation. This is evidenced by the fact that applying 0.7 V to pre-adsorbed ethane led to 2.6 times more methane than when carrying out both adsorption and C−C cleavage at 0.7 V (Figure S8). The higher yields are a result of overcoming the low adsorption observed at 0.7 V, by loading substrate on the electrode before leveraging the favorable C−C bond cleavage at 0.7 V. We expect that further tuning the potential and duration of the adsorption and scission steps will allow optimization of methane yield and selectivity.

Proposed mechanism of $C(sp^3)$−$C(sp^3)$ bond fragmentation

We propose that methane generation takes place through the transient formation of a non-desorbable surface intermediate. We observed evidence for this pathway both from time-dependent and potential-dependent fragmentation measurements, wherein we quantified the amount of ethane and methane produced after applying oxidative potentials to ethane adsorbed at 0.2 V. Varying the

duration during which we applied 0.5 V revealed that the consumption of ethane and production of methane proceed at different rates (**Figure 4b**). Specifically, the ethane yield decreased sharply within one minute and was reduced to trace amounts after 5 minutes, whereas the yield of methane increased as long as the oxidative potential was being applied. In addition, when quantifying the total amount of desorbable carbon atoms, we observed a decrease with time that reached a minimum at 5 minutes (Figure S9), while the total amount of adsorbed ethane was constant for each experiment (Figure S10). The asynchronous nature of ethane depletion and methane production, combined with the appearance of a minimum in desorbable alkanes, suggests a sequential fragmentation mechanism involving a non-desorbable intermediate, which could not be identified through EC-MS.

We further corroborated the presence of a non-desorbable intermediate by quantifying the total amount of ethane and methane produced after varying the *magnitude* of the oxidative potential applied to ethane adsorbed at 0.2 V. We found that subjecting the electrode to 0.4 V and 0.5 V decreased the total amount of methane and ethane compared to the case where no oxidative potential was applied (**Figure 5c**). This again indicates that part of the pre-adsorbed ethane transforms into a non-desorbable form under oxidative bias. However, under more oxidative conditions (0.6 V), the amount of reductively desorbable carbon sharply increased, suggesting that highly oxidative potentials facilitate the transformation of a non-desorbable adsorbate into reductively desorbable methane.

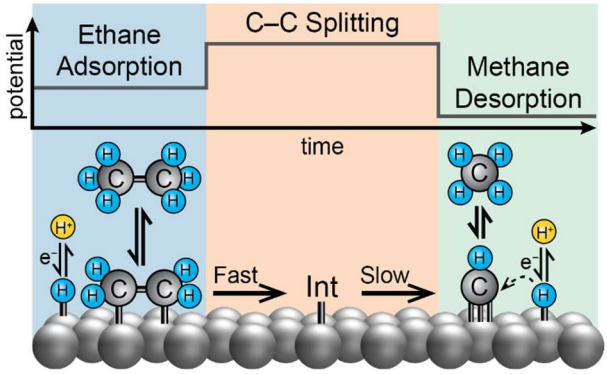

Figure 6. Schematic of hypothesized mechanism where the adsorbed ethane is rapidly converted to an active intermediate upon applying an oxidative potential. The intermediate undergoes a slow cleavage step to produce fragments that are reductively desorbed as methane.

Based on these findings, we theorize that C−C bond fragmentation involves the transformation of adsorbed ethane into a reductively non-desorbable surface intermediate (**Figure 6**). In a subsequent step, this intermediate undergoes fragmentation to produce C_1 compounds. Both steps are potential dependent, but the generation of the intermediate appears to occur at a faster rate than the C−C fragmentation event, explaining the transient decrease in the amount of total desorbable carbon. At 0.7 V, the total amount of desorbed carbon decreases, which is attributed to the generation of CO_2 (Figure S6). Our observations are consistent with the prevailing mechanistic hypothesis of thermal hydrogenolysis, which suggests that C−C bond cleavage requires the formation of a dehydrogenated intermediate which subsequently undergoes fragmentation.[32–35] While the

intermediate in our proposed pathway is consistent with this idea, alternative mechanisms including an overall oxidation reaction remain possible. Further mechanistic investigation will be necessary to understand how the electrode potential controls the formation and transformation of the proposed intermediates.

Discussion

Here, we demonstrate an electrocatalytic approach to cleave the $C(sp^3)-C(sp^3)$ bond in ethane at room temperature. Our findings are made possible by using time-dependent electrode potential sequences, combined with monolayer-sensitive in-situ analysis, allowing for independent investigation of ethane adsorption, C−C bond fragmentation, and methane desorption. Importantly, our approach allowed us to use variations in the electrode potential to promote the scission of ethane *while it is bound to the catalyst surface*, resulting in unprecedented control over the selectivity of this alkane transformation reaction, which cannot be accomplished under constant potentials. We further note that the use of time-dependent potentials can provide a methodology to study individual steps of an electrocatalytic reaction in isolation.

The methodology demonstrated herein provides novel avenues to steer catalytic reactions and demonstrates that these avenues can be exploited to gain astonishing control over the room-temperature electrocatalytic transformation of challenging substrates such as n-alkanes. We believe that the ability to independently control catalytic adsorption, transformation and desorption steps presents broad opportunities for generating fundamental insight into novel electrochemical reaction pathways of importance to energy storage and sustainable chemical transformations. Despite this promise, substantial future research efforts are required to refine this technology and address existing shortcomings. For example, applying strongly oxidative potentials after ethane adsorption and fragmentation experiments, led to the release of a substantial amount of CO_2 (Figure S11). This led us to conclude that, in addition to the formation of ethane and methane, adsorption of ethane on Pt leads to the formation of compounds that cannot be desorbed under reductive conditions. We hypothesize that these compounds correspond to oxidized alkane fragments,[21–25,29] the formation of which could potentially be suppressed through future materials engineering. Future research will have to investigate the impact of electrolytes in controlling the adsorption and fragmentation of alkanes, as well as the site-selectivity of fragmentation in long-chain alkanes, which in the long run could lead to electrochemical technologies for decomposing plastics such as polyethylene.

Steering the transformation of intermediates after their adsorption to the catalyst constitutes a missing lever of control in catalysis, which presently is primarily achieved through the manipulation of individual molecules using scanning tunneling microscopes.[36,37] Our findings therefore widen the parameter space for catalytic reaction engineering by demonstrating that electrochemical potentials can induce transformations of surface adsorbates on an extended surface. This approach opens the door to the electricity-driven transformation of $C(sp^3)-C(sp^3)$ and $C(sp^3)-H$ bonds in alkanes at room temperature, laying the groundwork for future sustainable synthesis and energy storage technologies.

Experimental Methods

Synthesis and Characterization of Platinized Pt Catalyst. A platinum stub (99.995%, Pine Instruments) was polished using alumina (0.3-0.05 μm diameter, Allied High Tech) and sonicated in Milli-Q H_2O twice for 15 min each. The stub was then plated with nanoporous Pt using a chronopotentiometric approach. Using a method from reported literature,[38] a solution of H_2PtCl_6 (0.072 mol L^{-1}, 99.9% trace metals basis, Sigma Aldrich) and 0.13 mmol L^{-1} $Pb(C_2H_3O_2)_2$ (99.999% trace metals basis, Sigma Aldrich) in Milli-Q H_2O (>18.2 MΩ) was contacted with a Pt stub (99.995%, Pine Instruments) working electrode, Pt wire (99.999%, Sigma Aldrich) counter, and a Ag/AgCl | 3 mol L^{-1} KCl reference (BASi) and 10 mA/cm^2 passed for 10 min. The platinized Pt stub was then dipped in Milli-Q H_2O several times to remove any residual solvated Pt ions before use.

The electrochemical surface area (ECSA) was measured by the underpotential deposition of a Cu monolayer at 0.2 V (Ag/AgCl NaCl 3 mol L^{-1}) for 3 min using 5 mol L^{-1} $CuSO_4$ (ACS Reagent, Sigma Aldrich) in 0.1 mol L^{-1} $HClO_4$ (ACS Reagent, Sigma Aldrich) followed by oxidation using a linear sweep at 100 mV s^{-1} up to 1.2 V. The background-subtracted oxidation currents were then integrated to give the charge passed, which was converted to surface area using 420 μC cm^{-2} as the correlation.[39]

Zeiss LEO 1530 and Zeiss Gemini 450 scanning electron microscopes (SEMs) were employed for measuring the morphology of the platinized electrodes. The images were acquired under an acceleration voltage of 3 kV using the in-lens detector.

MS Measurements. All measurements were taken using an EC-cell constructed out of Kel-F perfluorinated polymer with compartments for the working, counter, and reference electrodes. The cell was mounted onto a semipermeable membrane chip (Spectro Inlets, Denmark) interfaced with the MS to allow products to diffuse through the chip and into the MS, enabling real-time detection of desorbed products. The MS was operated using Zilien Software (Spectro Inlets, Denmark)

Electrochemical Measurements. All experiments were performed using a Biologic SP-200 potentiostat controlled with EC-lab software with a three-electrode assembly consisting of a platinized Pt working electrode, Pt wire counter, and Ag/AgCl | 3 mol L^{-1} KCl reference electrode. To compensate for the solution resistance, 85% software-based impedance measurement technique (ZIR) was used for IR drop compensation.

H_2SO_4 (1 mol L^{-1}, Macron ACS Reagent) electrolyte was used and was degassed with He sparging for 15 min prior to injection into the EC cell. The EC cell was cleaned with piranha solution (75% H_2SO_4, 25% H_2O_2), rinsed with Milli-Q water, and dried with compressed air prior to each experiment to avoid organic contamination.

The experiments were performed by stepping the potential through the predetermined set points for a controlled amount of time using EC-lab. Adsorption was performed by applying the desired potential for 30 min under ethane flow, followed by 15 min of He flow to remove the substrate from the system. Desorption was then performed under He by first stepping reductively to 0.05 V for 10 min then removing the remaining adsorbates by complete oxidation at 1.2 V for 10 min.

Acknowledgements: Support for this research was provided by the University of Wisconsin - Madison Office of the Vice Chancellor for Research and Graduate Education. The authors gratefully acknowledge the use of facilities and instrumentation at the UW-Madison Wisconsin Centers for Nanoscale Technology (wcnt.wisc.edu). Lastly, we thank Prof. Manos Mavrikakis and Prof. George Huber for helpful input. **Funding:** This work was performed with funding from the Wisconsin Alumni Research Foundation. This material is based upon work supported by the National Science Foundation Graduate Research Fellowship Program under Grant No. DGE-1747503. Any opinions, findings, and conclusions or recommendations expressed in this material are those of the authors and do not necessarily reflect the views of the National Science Foundation. Instrumentation for this research was partially supported by the NSF through the University of Wisconsin Materials Research Science and Engineering Center (DMR-1720415).
Author Contributions: Co-first authors are listed in alphabetical order. M. S. and C. L. designed the project and experiments. H. B. B. designed and performed experiments. H-S. C. performed electron microscopy and contributed to surface area measurements. C. L., H. B. B., M. S. and H-S. C. analyzed data and wrote the manuscript. M. S. was responsible for supervision, funding acquisition, and project administration. **Competing Interests:** The authors declare no competing interests. **Data and Materials Availability:** All data and images are available in the manuscript or the supplementary information.

REFERENCES

1. Raciti, D. & Wang, C. Recent Advances in CO_2 Reduction Electrocatalysis on Copper. *ACS Energy Lett.* **3**, 1545–1556 (2018).
2. Nitopi, S. *et al.* Progress and Perspectives of Electrochemical CO_2 Reduction on Copper in Aqueous Electrolyte. *Chem. Rev.* **119**, 7610–7672 (2019).
3. Klein, C. K. & Manthiram, K. Sustainable ammonia synthesis: Just around the corner? *Joule* **6**, 1971–1973 (2022).
4. Suryanto, B. H. R. *et al.* Nitrogen reduction to ammonia at high efficiency and rates based on a phosphonium proton shuttle. *Science* **372**, 1187–1191 (2021).
5. Zhu, C., Ang, N. W. J., Meyer, T. H., Qiu, Y. & Ackermann, L. Organic Electrochemistry: Molecular Syntheses with Potential. *ACS Cent. Sci.* **7**, 415–431 (2021).
6. Lucky, C., Wang, T. & Schreier, M. Electrochemical Ethylene Oxide Synthesis from Ethanol. *ACS Energy Lett.* 1316–1321 (2022).
7. Daehn, K. *et al.* Innovations to decarbonize materials industries. *Nat. Rev. Mater.* **7**, 275–294 (2021).
8. van Geem, K. M., Galvita, V. v. & Marin, G. B. Making chemicals with electricity. *Science* **364**, 734–735 (2019).
9. Schiffer, Z. J. & Manthiram, K. Electrification and Decarbonization of the Chemical Industry. *Joule* **1**, 10–14 (2017).
10. Sabatier, P. *La Catalyse En Chimie Organique*. (Nouveau Monde, 1920). doi:10.14375/NP.9782369430186.

11. Boudart, M. & Djega-Meriadassou, G. *Kinetics of Heterogeneous Catalytic Reactions*. (Princeton University Press, 1984).
12. Gopeesingh, J. *et al.* Resonance-promoted formic acid oxidation via dynamic electrocatalytic modulation. *ACS Catal.* **2020**, 9932–9942 (2020).
13. Baz, A., Lyons, M. & Holewinski, A. Dynamic electrocatalysis: Examining resonant catalytic rate enhancement under oscillating electrochemical potential. *Chem. Catalysis* **2**, 3497–3516 (2022).
14. Shetty, M. *et al.* The Catalytic Mechanics of Dynamic Surfaces: Stimulating Methods for Promoting Catalytic Resonance. *ACS Catal.* **10**, 12666–12695 (2020).
15. Ardagh, M. A. *et al.* Catalytic resonance theory: parallel reaction pathway control. *Chem. Sci*. **11**, 3501–3510 (2020).
16. Ardagh, M. A., Birol, T., Zhang, Q., Abdelrahman, O. A. & Dauenhauer, P. J. Catalytic resonance theory: superVolcanoes, catalytic molecular pumps, and oscillatory steady state. *Catal. Sci. Technol.* **9**, 5058–5076 (2019).
17. Dauenhauer, P. J., Shetty, M., Ardagh, M. A., Pang, Y. & Abdelrahman, O. A. Electric-field-assisted modulation of surface thermochemistry. *ACS Catal.* **10**, 12867–12880 (2020).
18. Kim, C., Weng, L. C. & Bell, A. T. Impact of Pulsed Electrochemical Reduction of CO_2 on the Formation of C_{2+} Products over Cu. *ACS Catal.* **10**, 12403–12413 (2020).
19. Trimarco, D. B. *et al.* Enabling real-time detection of electrochemical desorption phenomena with sub-monolayer sensitivity. *Electrochim. Acta* **268**, 520–530 (2018).
20. Baltruschat, H. Differential electrochemical mass spectrometry. *J. Am. Soc. Mass Spectrom.* **15**, 1693–1706 (2004).
21. Niedrach, L. W. & Tochner, M. Studies of Hydrocarbon Fuel Cell Anodes by the Multipulse Potentiodynamic Method. *J. Electrochem. Soc.* **114**, 233 (1967).
22. Bruckenstein, S. & Comeau, J. Electrochemical Mass Spectrometry Part 1 .-Preliminary Studies of Propane Oxidation on Platinum. *Faraday Discuss. Chem. Soc.* **91**, 285–292 (1973).
23. Barger Jr., H. J. & Savitz, M. L. Chemical Identification of Adsorbed Species in Fuel Cell Reactions I. Propane Oxidation. *J. Electrochem. Soc.* **115**, 686–690 (1968).
24. Brummer, S. B., Ford, J. I. & Turner, M. J. The Adsorption and Oxidation of Hydrocarbons on Noble Metal Electrodes. I. Propane Adsorption on Smooth Platinum Electrodes. *J. Phys. Chem.* **69**, 3424–3433 (1965).
25. Brummer, S. B. Oxidation and Adsorption of Hydrocarbons on Noble Metal Electrodes VI. A Discussion of the Mechanism of Saturated Hydrocarbon Oxidation on Platinum. in *Fuel Cell Systems - II* (ed. Gould, R. F.) 223–230 (American Chemical Society, 1969).
26. Gilman, S. Studies of Hydrocarbon Surface Processes by the Multipulse Potentiodynamic Method Part 2.-Kinetics and Mechanism of Desorption of Ethane from Platinum. *J. Chem. Soc. Faraday Trans.* **61**, 2561–2568 (1965).
27. Niedrach, L. W. Galvanostatic and Volumetric Studies of Hydrocarbons Adsorbed on Fuel Cell Anodes. *J. Electrochem. Soc.* **111**, 1309–1317 (1964).

28. Gilman, S. Studies of Hydrocarbon Surface Processes by the Multipulse Potentiodynamic Method Part 1.-Kinetics and Mechanisms of Ethane Adsorption on Platinum. *J. Chem. Soc. Faraday Trans.* **61**, 2546–2560 (1965).
29. Solis, V., Castro Luna, A., Triaca, W. E. & Arvfa, A. J. The Electrosorption and the Potentiodynamic Electrooxidation of Ethane on Platinum at Different Temperatures. *J. Electrochem. Soc.* **128**, 2115–2122 (1981).
30. Cortright, R. D., Watwe, R. M., Spiewak, B. E. & Dumesic, J. A. Kinetics of ethane hydrogenolysis over supported platinum catalysts. *Catal. Today* **53**, 395–406 (1999).
31. Climent, V., García-Araez, N., Herrero, E. & Feliu, J. Potential of zero total charge of platinum single crystals: A local approach to stepped surfaces vicinal to Pt(111). *Russ. J. Electrochem.* **42**, 1145–1160 (2006).
32. Almithn, A. & Hibbitts, D. Comparing Rate and Mechanism of Ethane Hydrogenolysis on Transition-Metal Catalysts. *J. Phys. Chem. C* **123**, 5421–5432 (2019).
33. Hibbitts, D. D., Flaherty, D. W. & Iglesia, E. Role of Branching on the Rate and Mechanism of C-C Cleavage in Alkanes on Metal Surfaces. *ACS Catal.* **6**, 469–482 (2016).
34. Hibbitts, D. D., Flaherty, D. W. & Iglesia, E. Effects of Chain Length on the Mechanism and Rates of Metal-Catalyzed Hydrogenolysis of n-Alkanes. *J. Phys. Chem. C* **120**, 8125–8138 (2016).
35. Flaherty, D. W., Hibbitts, D. D., Gürbüz, E. I. & Iglesia, E. Theoretical and kinetic assessment of the mechanism of ethane hydrogenolysis on metal surfaces saturated with chemisorbed hydrogen. *J. Catal.* **311**, 350–356 (2014).
36. Zhao, A. *et al.* Physics: Controlling the Kondo effect of an adsorbed magnetic ion through its chemical bonding. *Science* **309**, 1542–1544 (2005).
37. Imada, H. *et al.* Real-space investigation of energy transfer in heterogeneous molecular dimers. *Nature* **538**, 364–367 (2016).
38. Feltham, A. M. & Spiro, M. Platinized platinum electrodes. *Chem. Rev.* **71**, 177–193 (1971).
39. Chen, H. S. *et al.* Preserving the Exposed Facets of Pt_3Sn Intermetallic Nanocubes during an Order to Disorder Transition Allows the Elucidation of the Effect of the Degree of Alloy Ordering on Electrocatalysis. *J. Am. Chem. Soc.* **142**, 3231–3239 (2020).